Optics Letters

High-resolution Cs–Rb two-photon spectrometer for directly stabilizing a Ti:sapphire comb laser

Tze-Wei Liu,[1,2] Bo-Wei Chen,[1,3,4] Hsin-Hung Yu,[1] and Wang-Yau Cheng[1,*]

[1]Department of Physics, National Central University, Taoyuan City 32001, Taiwan
[2]Trapped-Ion Quantum Computing Laboratory, Hon Hai Research Institute, Taipei 11492, Taiwan
[3]Molecular Sciences and Technology, Taiwan International Graduate Program, Academia Sinica, National Central University, Taipei, Taiwan
[4]Institute of Atomic and Molecular Science, Academia Sinica, Taipei 11529, Taiwan
*Wycheng@phys.ncu.edu.tw

Received 2 February 2023; revised 5 March 2023; accepted 19 March 2023; posted 28 March 2023; published 27 April 2023

In this paper, we present a simple scheme for efficiently removing the residual Doppler background of a comb laser based two-photon spectrometer to be better than 10^{-3} background-to-signal ratio. We applied this scheme to stabilize the frequencies of a mode-locked Ti:sapphire laser directly referring to the cesium 6S–8S transition and rubidium 5S–5D transition. We suggest a standard operation procedure (SOP) for the fully direct comb laser stabilization and evaluate the frequency of two spectral lines at a certain temperature, by which we demonstrate an all-atomic-transition-based Ti:sapphire comb laser merely via a 6-cm glass cell.

https://doi.org/10.1364/OL.486825

The Ti:sapphire (Ti:S) laser possesses unique features of broadband laser spectrum and high laser-power damage threshold with low phase noise, and hence plays a key role in frontier sciences like high-field physics [1], attosecond science [2], extreme UV (EUV) comb generation [3], and so on. To equip a mode-locked laser to become a comb laser, people usually use a "self-reference" scheme via nonlinear optics [4–9] to lock the laser offset frequency (f_{offset}) and one more clock either recognized by BIPM [10–12] or some other reliable optical references [13–17] to lock the repetition rate (f_{rep}). Directly locking a Ti:S comb laser to atomic transitions is a new trend benefiting "simplicity", "directly referring to atomic transition", and "being cost-effective". Yet, to our knowledge, only a few experiments demonstrated direct comb frequency locking [14,16,17] to only one parameter of the comb laser (f_{rep}), whereas no comb laser stabilization fully refers the two parameters (f_{offset}, f_{rep}) to atomic transitions, not to mention the error analysis on this sort of comb clock. In this paper, a simple setup for direct frequency comb spectroscopy (DFCS) is presented without the problem of residual Doppler background, and by which we realize a novel atomic-transition-based Ti:S comb laser and the discussion of comb frequency errors. The scheme presented here is simple, with no need for any nonlinear optics nor an additional optical clock.

The relevant level diagrams of atomic transitions are illustrated on the left-hand side of Fig. 1, with the right-hand side showing our Cs–Rb spectrometer. A compact Ti:S laser (25 cm × 50 cm) having the specifications of 1-GHz repetition rate, 45-femtosecond pulse, and 800-nm central wavelength is implemented as the light source of our Cs–Rb spectrometer. The double-pass acousto-optic modulator (AOM) shown in Fig. 1 is mainly for investigating the AC Stark shifts and for enlarging the tuning range of the laser offset frequency (f_{offset}). After the laser beam passes through one broadband Fresnel rhomb, the counter-propagating light pulses of left circular polarization are presented in the atomic system. The fluorescence from cesium atoms at the $8S_{1/2}$ level (~460 nm) and rubidium atoms at the $5D_{3/2}$ level (~420 nm) are independently detected by two separate photomultiplier tubes (PMTs) with two separate interference filters (IFs), which provide evidence of the stepwise two-photon transitions illustrated by the level diagram in Fig. 1. Some other schemes [18,19] can also lead to similar Doppler-free spectra, while our uniqueness is collinear without a need to sacrifice any laser spectra with which our scheme benefits for building up a wideband and handy spectrometer. Figure 2 displays high-resolution Cs–Rb spectroscopy resolved by our spectrometer in Fig. 1 in which no residual Doppler background was found except for that represented by the orange curve. The f_{offset} in Fig. 2 was kept at 820.3 MHz by offset locking one comb mode [20] against a cesium stabilized 822-nm diode [21]. The beat frequency Δf between two lasers is tunable by an electric-optical modulator (EOM) mentioned in Ref. [21]. To resolve the spectra in Fig. 2, the "Δf" was changed correspondingly with the change of repetition rate to keep the f_{offset} constant. The Doppler-free spectra (blue lines) in Fig. 2 were obtained by constantly varying the direction of the retro-reflected beam by the piezoelectric transducer (PZT) shown in Fig. 1, with 150-Hz modulation frequency that is much faster than the scan rate in Fig. 2. Since the residual Doppler background mainly comes from the one-way self-stepwise transition, modulating the PZT length can extract the part of fluorescence originating from only the overlapped pulses and keep the background unmodulated, through which we eliminated the spectral background to be less than 10^{-3} background-to-signal ratio. This is proved by the comparison between orange and blue curves in Fig. 2 in which the instrument ground line (red dashed line) and the spectra baseline were indistinguishable. The two blue curves in Fig. 2, namely the Rb and Cs spectra, were resolved simultaneously and the f_{rep} was tuned at a rate of 1 Hz/sec. We stopped activating the PZT and

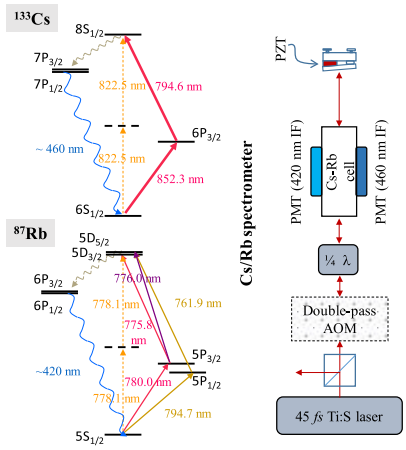

Fig. 1. Simple setup for a comb-laser based high-resolution Cs/Rb two-photon spectrometer, with the relevant level diagrams illustrated on the left-hand side. ¼ λ, quarter-wave plate; the double-pass AOM could be bypassed when in laser stabilization (see the text for details).

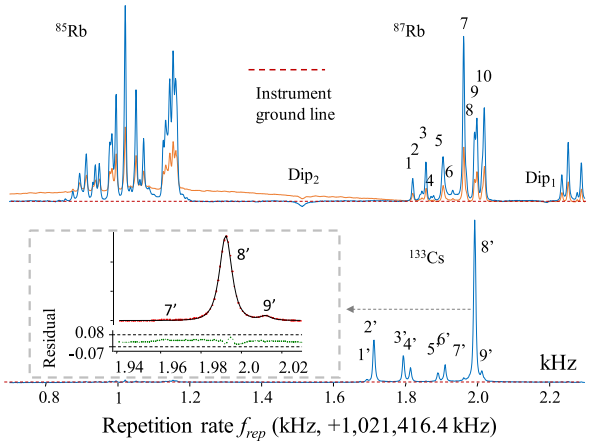

Fig. 2. Part of our direct frequency comb spectroscopy with Rb–Cs spectra resolved simultaneously (two blue curves); refer to Table 1 for the physics of line 7 and line 8' and the nearby lines. The orange line is another scan on the Rb spectra without activating the PZT in Fig. 1 for comparison. Comb laser offset frequency, 820.3 MHz; repetition rate scanning speed, 1 Hz per second. Dashed inset shows the enlarged line 8' with Lorentian-transit time line shape fitting [22].

re-scanned the spectra while keeping the other conditions all the same, under which the Rb spectra became different, as shown by the orange curve in Fig. 2. The assignments of the spectral lines in Fig. 2 are listed in Table 1. Only the lines relevant to what have been chosen for laser stabilization are addressed, namely the line 7 and line 8' and their nearby weak lines. Each cesium line in Table 1 contains two pathways because the ninth harmonic of our repetition rate is near (but not exactly equal to) the cesium clock frequency which is 9,192,631.770 kHz. This arrangement on f_{rep} enhances the blue fluorescence (~460 nm) while avoiding the disturbance of the possible coherent population trapping (CPT) if some buffer gas was added in the future. The enlarged line 8' displayed in the dashed box inset of Fig. 2 is to show the excellent agreement with the Lorentzian-transit time line shape fitting [22,23]. Our high-resolution scheme in this paper not only can

Table 1. Physics of Line 7 and Line 8', and the Nearby Lines

Lines in Fig. 2	Transition Pathways	Velocity[a]
^{87}Rb line 6	$5S_{1/2}\ F=1 \rightarrow 5P_{3/2}\ F=2 \rightarrow 5D_{3/2}\ F=3$	172.2 (ms^{-1})
^{87}Rb line 7	$5S_{1/2}\ F=1 \rightarrow 5P_{3/2}\ F=2 \rightarrow 5D_{5/2}\ F=3$	181.2 (ms^{-1})
^{133}Cs line 7'	$6S_{1/2}\ F=3 \rightarrow 6P_{3/2}\ F=2 \rightarrow 8S_{1/2}\ F=3$	192.4 (ms^{-1})
^{133}Cs line 8'	$6S_{1/2}\ F=4 \rightarrow 6P_{3/2}\ F=3 \rightarrow 8S_{1/2}\ F=3$ $^{*}6S_{1/2}\ F=3 \rightarrow 6P_{3/2}\ F=3 \rightarrow 8S_{1/2}\ F=3$	317.1 (ms^{-1})
^{133}Cs line 9'	$^{a}6S_{1/2}\ F=4 \rightarrow 6P_{3/2}\ F=4 \rightarrow 8S_{1/2}\ F=3$ $6S_{1/2}\ F=3 \rightarrow 6P_{3/2}\ F=4 \rightarrow 8S_{1/2}\ F=3$	482.5 (ms^{-1})

[a]The corresponding Doppler shift resonates with the transition

tell the difference between different species of atoms in terms of the transit time linewidth, but also leads to an awareness of quantum interference such as the intriguing Dip_1 and Dip_2 lines in Fig. 2. The Dip_1 comes from the two-pathway interference of ^{87}Rb $5S_{1/2} \rightarrow 5P_{1/2} \rightarrow 5D_{3/2}$ and $5S_{1/2} \rightarrow 5P_{3/2} \rightarrow 5D_{3/2}$, and the Dip_2 is from the V-type electromagnetic induced transparency (EIT) of ^{85}Rb $5S_{1/2} \rightarrow 5P_{3/2}$ and $5S_{1/2} \rightarrow 5P_{1/2}$. Those pathways were further confirmed by using an additional spatial light modulator (not shown in Fig. 1) to control the composition of the laser wavelengths.

We propose here a standard operation procedure (SOP) for activating our spectrometer to stabilize the comb laser frequencies. First, we choose two lines to overlap each other like what we demonstrated in Fig. 3(a). We chose spectral line 7 and line 8' at 95°C cell temperature and at 20-mW comb laser power because their SNR/linewidth is similar, where SNR stands for signal-to-noise ratio. Aligning the two lines could be realized by manually adjusting f_{rep} and f_{offset} such that the two lines were as close to each other as possible, though the peak positions of the two lines are not exactly equal. The next step is to precisely determine the resonant repetition rate (f^0_{rep}) and the resonant offset frequency (f^0_{offset}) at the condition of "two-line overlapping". Let Δf_{offset} stand for the detuning from f^0_{offset}, which could be obtained by curve fitting the entire spectra of the inseparable line 7 and line 8'. In our fitting, the linewidths of the two lines are always kept constant and are given by the approach demonstrated in the inset of Fig. 2. Figure 3(b) is the experimental data showing the relation between Δf_{offset} and f_{rep}. Each data point and the corresponding error bar were obtained from ten scans on f_{offset} under a fixed f_{rep} guessed in the first step. We then used the five data points in Fig. 3(b) to perform interpolation for deriving

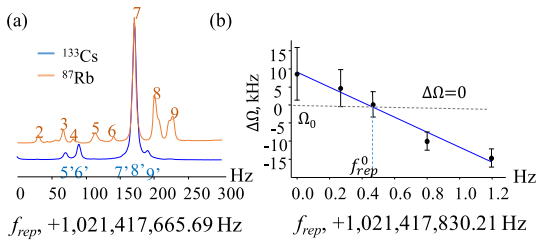

Fig. 3. Determining the f^0_{offset} and the f^0_{rep} at the condition of "two-line overlapping" (see the text for details). (a) Manually overlapping two lines. (b) Measured Δf_{offset} at different f_{rep} so that one can interpolate out (f^0_{rep}, f^0_{offset}); $\Delta f_{offset} = f_{offset} - f^0_{offset}$.

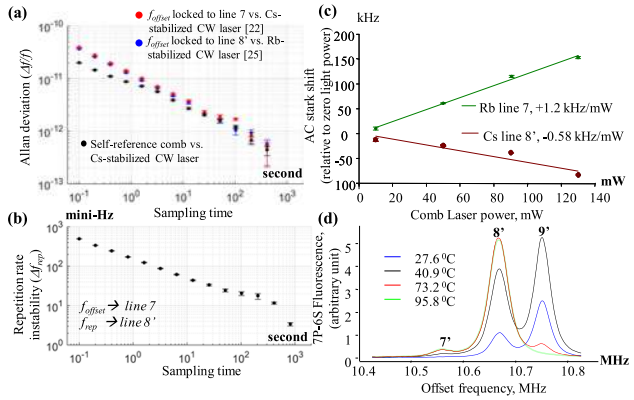

Fig. 4. (a) Comparisons between a *1f–2f* comb laser [4] and the comb laser whose offset frequency directly referring to line 7 or line 8', via two specific CW lasers. The comb laser repetition rates were all locked against a cesium atomic beam clock [25]. (b) Repetition rate instability as all comb laser parameters directly locked to atomic two-photon transitions, see the text. (c) AC Stark shifts of line 7 and line 8'. (d) Line pulling by the nearby lines of line 8' versus cell temperature.

the f^0_{offset} at zero-Δf_{offset}. Next, we fixed the comb laser offset frequency at f^0_{offset} and scanned the f_{rep} to obtain the f^0_{rep}. The f^0_{rep} Zwas found to be 1,021,417,830.69 ± 0.03 Hz; the f^0_{offset} was found to be 1,020,412 ± 5 kHz; the velocity of cesium and rubidium were 311.1 m/s and 181.5 m/s, respectively, under the conditions of 20 ± 0.002-mW average power and 95°C cell temperature. The frequencies agree well with what have been measured in Ref. [23] and Refs. [10,24] within 15-kHz uncertainty which includes the estimate of He-diffusion [23]. The final step is to replace the aforementioned Cs-stabilized 822-nm diode laser by directly stabilizing the f^0_{offset} to line 8' and, meanwhile, to replace the Cs atomic beam clock [25] by a signal generator inside which the voltage-controlled oscillator (VCO) was frequency stabilized via line 7 and hence the f^0_{rep} was stabilized. In this paper, the Cs atomic beam clock was used for stabilizing the comb laser repetition rate except for the experiment performed in Fig. 4(b). One field programmable gate array (FPGA)-chip based development board [26], which costs 100 USD in the year 2020, was enough to realize comb laser stabilization. The above SOP of determining f^0_{offset} and f^0_{rep} is vital for some pair of spectral lines whose "two-lines overlapping" frequency was never measured before. Moreover, in terms of preparing a high-accurate frequency comb, the AOM in Fig. 2 is not needed to reduce the error sources.

By the SOP mentioned above, we claim that the repetition rate and offset frequency must be uniquely defined since, once the comb laser frequency is stabilized to line 8', the frequencies of two specific comb modes always meet the following criteria:

$$f^{794}_{Cs} = f^{794}_{n'}\left(1-\frac{v'}{c}\right) = (n' f_{rep} + f_{offset})\left(1-\frac{v'}{c}\right), \quad (1)$$

$$f^{852}_{Cs} = f^{852}_{m'}\left(1+\frac{v'}{c}\right) = (m' f_{rep} + f_{offset})\left(1+\frac{v'}{c}\right). \quad (2)$$

The relation between f^{794}_{Cs} and f^{852}_{Cs} is illustrated in the level diagram of Fig. 1 as

$$f^{794}_{Cs} + f^{852}_{Cs} = 2f^{822.5}_{Cs}, \quad (3)$$

where the mode numbers *n'* and *m'* are 369,372 and 344,355, respectively; f^{852}_{Cs} stands for the transition frequency of cesium $6S_{1/2}(F=3) \rightarrow 6P_{3/2}(F=3)$ whose frequency has been measured by the Max Planck Garching group [15] by frequency chain and the NIST Boulder group [16] by DFCS; f^{794}_{Cs} stands for the transition frequency of cesium $6P_{3/2}(F=3) \rightarrow 8S_{1/2}(F=3)$, which could be derived either from the Taiwan NCU group [23] by CW laser measurement or from the Max Planck Garching group [27] by DFCS; and $f^{794}_{n'}$ and $f^{852}_{m'}$ are the corresponding comb-mode frequencies. When Eqs. (1)–(3) are satisfied with a coherent stepwise two-photon transition (STPT), the transition rate from $6S_{1/2}(F=3)$ to $8S_{1/2}(F=3)$ was dramatically enhanced [28] compared to that of the direct two-photon transition (DTPT) [19]. However, this advantage is not beneficial for a comb-laser-based optical standard because the atom's velocity is not fixed which will lead to a variable f_{offset}, depending on different f_{rep}. The dilemma of "high spectral resolution but uncertain f_{offset}", pointed out by Eikema [19], was solved in this paper as we added one more atom species in the same gas cell. That is, more criteria are imposed as

$$f^{776}_{Rb} = f^{776}_{n}\left(1-\frac{v}{c}\right) = (n f_{rep} + f_{offset})\left(1-\frac{v}{c}\right), \quad (4)$$

$$f^{780}_{Rb} = f^{780}_{m}\left(1+\frac{v}{c}\right) = (m f_{rep} + f_{offset})\left(1+\frac{v}{c}\right), \quad (5)$$

where the relation between f^{776}_{Rb} and f^{780}_{Rb} is illustrated in the level diagram of Fig. 1 as

$$f^{776}_{Rb} + f^{780}_{Rb} = 2f^{778.1}_{Rb}. \quad (6)$$

The other notation in Eqs. (4)–(6) have similar meanings to those in Eqs. (1)–(3), and the mode numbers *m* and *n* are 378,239 and 376,177, respectively. The Rb two-photon clock has been recommended by BIPM [10], and its intermediate states have been precisely measured by the J. Hall group. [29]. Once line 7 and line 8' are forced to overlap, together with the criteria of integer mode numbers between two stepwise wavelengths, it will lead to a unique solution of Eqs. (1)–(6). The accuracies of the frequencies of f^{852}_{Cs}, f^{780}_{Rb}, $2f^{822.5}_{Cs}$, $2f^{778.1}_{Rb}$ are thus vital for examining our SOP mentioned previously and that is the main reason for choosing the Rb $5S_{1/2}$–$5D_{3/2}$ stepwise transition and the Cs $6S_{1/2}$–$8S_{1/2}$ stepwise transition to be the frequency references in this paper. The frequency instability and inaccuracy in Fig. 4 are inspected by one Cs-stabilized 822-nm CW laser [21,23] and one Rb-stabilized 778-nm CW laser [10,24], as their frequencies have been sophisticatedly studied for decades. Figure 4(a) proves that some self-reference schemes via nonlinear optics [4–9] could be replaced by merely one 6-cm glass cell without losing the laser stability by comparing with that of a *1f–2f* self-referenced comb laser [4]. Figure 4(b) shows the instability of the repetition rate when we stabilized both f_{offset} and f_{rep} directly to the line center of line 8' and line 7, respectively. Using an FPGA to search the signal peak can avoid a constant modulation on the comb laser, whereas we still have the problem of incorporating a long-term integrator into the FPGA algorithm, therefore we did not present the long-term Allan variance in this study.

We investigate two main frequency errors for studying the frequency of our atomic transitions-based comb laser. That is, AC Stark shift and cell-temperature-induced shift. The AC Stark shift in cesium is almost the same as what has been reported by either a CW laser [21] or comb laser [27], whereas the rubidium atom exhibits a blueshift that is even an opposite shift to

Table 2. Influence of Cell Temperature on the Locking Frequency of Line 7 and Line 8'[a]

Cell/Cold Finger (°C)	Line 7[b] Shift (kHz)	Line 7[c] Width (MHz)	Line 8'[b] Shift (kHz)	Line 8'[c] Width (MHz)
95.8/77.4	0	1.86 (4)	0	2.21 (4)
74.0/61.9	45 (4)	1.36 (6)	10 (6)	2.15 (2)
53.6/47.5	62 (3)	1.35 (6)	-67 (10)	1.75 (6)
26.1/26.1	20 (3)	1.5 (1)	-123 (8)	1.52 (8)

[a]Relative to our suggested temperature (see the text for details).
[b]Relative to that at 74°C, at which comb laser is stabilized.
[c]FWHM resolved simultaneously.

what has been measured by a CW laser (redshift, [24]). The frequency shift caused by cell temperature in Table 2 comes from two physical mechanisms: one is from the atom collisions and the other is from the pulling effect by nearby lines as illustrated in Fig. 4(d). In terms of collisions, we note that there are two transition pathways in line 8' (see Table 1) and two species of atoms involved in the collision process that add complexity in data analysis. In terms of line pulling, there are two effects competing the line strengths in Fig. 4(d), that is, the atom numbers changed with vapor pressure and the Beer's-law-induced mode power attenuation. When the cell was heated up to 95.8°C, the line 8' grew up with the increase of atom numbers while the line 9' is invisible as shown by the green curve in Fig. 4(d). However, as the cell temperature was set to be lower than 40°C (black and blue curves), the line strength of line 9' could even be larger than that of line 8'. We conclude that the frequency shift is less sensitive at around 95°C. The third notable error source is the Zeeman shift, which is negligible here since we have reduced the Earth's magnetic field at the fluorescence detection area to be below one mini-gauss by three independent pairs of Helmholtz coils [30].

To summarize, we not only present a high-resolution and clean-background Rb–Cs two-photon spectrometer, but also demonstrate the feasibility of an all-atomic-transition based Ti:S comb laser via merely one 6-cm glass cell, with which we no longer need a self-reference scheme for locking f_{offset} nor need an additional clock for locking f_{rep}. This paper also reveals some interesting issues in the comb laser–atom interaction so that the physics is worthy of further study, such as the abnormal AC Stark shift in line 7 as shown in Fig. 4(c), the non-monotonical change on the frequency shift versus cell temperature for line 7 and line 8' as shown in Table 2, the transition phases of Dip_1 line and Dip_2 line, and so on.

Acknowledgment. We are grateful for the precious comments of Professor John L. Hall in JILA on this work. The MATLAB program was amended from what is generously provided by Prof. Jason E. Stalnaker in Oberlin College. We thank Mr. Guan-Wei Hu for the line shape fitting program and Mr. Ko-Han Chen and Mr. Yu-Jhe Shih for operating all the CW lasers. We also thank Mr. Po-Chen Chang in Chunghwa Telecom Laboratories for lending us the cesium atomic beam clock.

Disclosures. The authors declare no conflicts of interest.

Data availability. Data underlying the results presented in this Letter are not publicly available at this time but may be obtained from the authors upon reasonable request.

REFERENCES

1. A. J. Gonsalves, K. Nakamura, and J. Daniels, *et al.*, Phys. Rev. Lett. **122**, 084801 (2019).
2. K.-Y. Chang, L.-C. Huang, K. Asaga, M.-S. Tsai, L. Rego, P.-C. Huang, H. Mashiko, K. Ogure, C. Hernanddez-Garcia, and M.-C. Chen, Optica **8**, 484 (2021).
3. I. Pupeza, C. Zhang, M. Högner, and J. Ye, Nat. Photonics **15**, 175 (2021).
4. D. J. Jones, S. A. Diddams, J. K. Ranka, A. Stentz, R. S. Windeler, J. L. Hall, and S. T. Cundiff, Science **288**, 635 (2000).
5. T. Fuji, A. Apolonski, and F. Krausz, Opt. Lett. **29**, 632 (2004).
6. Y. Okawachi, M. Yu, J. Cardenas, X. Ji, A. Klenner, M. Lipson, and A. L. Gaeta, Opt. Lett. **43**, 4627 (2018).
7. T. I. Ferreiro, J. Sun, and D. T. Reid, Opt. Lett. **35**, 1668 (2010).
8. D. Fehrenbacher, P. Sulzer, A. Liehl, T. Kälberer, C. Riek, D. V. Seletskiy, and A. Leitenstorfer, Optica **2**, 917 (2015).
9. S. Okubo, A. Onae, K. Nakamura, T. Udem, and H. Inaba, Optica **5**, 188 (2018).
10. BIPM, http://www.bipm.org/en/publications/mises-en-pratique/standard-frequencies.html.
11. M. Lezius, T. Wilken, and C. Deutsch, *et al.*, Optica **3**, 1381 (2016).
12. L. S. Ye, J. L. Ma, and Hall, Phys. Rev. Lett. **87**, 270801 (2001).
13. W.-Y. Cheng, T. H. Wu, S. W. Huang, S. Y. Lin, and C. M. Wu, Appl. Phys. B **92**, 13 (2008).
14. L. Stern, J. R. Stone, S. Kang, D. C. Cole, M.-G. Suh, S. A. Diddams, and S. B. Papp, Sci. Adv. **6**, eaax6230 (2020).
15. T. Udem, J. Reichert, T. W. Hänsch, and M. Kourogi, Phys. Rev. A **62**, 031801 (2000).
16. V. Gerginov, C. E. Tanner, S. A. Diddams, A. Bartels, and L. Hollberg, Opt. Lett. **30**, 1734 (2005).
17. S. Y. Zhang, J. T. Wu, Y. L. Zhang, J. X. Leng, W. P. Yang, Z. G. Zhang, and J. Y. Zhao, Sci. Rep. **5**, 15114 (2015).
18. J. E. Stalnaker, V. Mbele, V. Gerginov, T. M. Fortier, S. A. Diddams, L. Hollberg, and C. E. Tanner, Phys. Rev. A **81**, 043840 (2010).
19. S. Barmes, Phys. Rev. Lett. **111**, 023007 (2013).
20. W.-Y. Cheng, T.-J. Chen, C.-W. Lin, B.-W. Chen, Y.-P. Yang, and H. Y. Hsu, Opt. Express **25**, 2752 (2017).
21. C. M. Wu, T. W. Liu, M. H. Wu, R. K. Lee, and W. Y. Cheng, Opt. Lett. **38**, 3186 (2013).
22. F. Biraben, M. Bassini, and B. Cagnac, J. Phys. **40**, 445 (1979).
23. K. H. Chen, C. M. Wu, S. R. Wu, H. H. Yu, T. W. Liu, and W. Y. Cheng, Opt. Lett. **45**, 4088 (2020).
24. C. S. Edwards, G. P. Barwood, H. S. Margolis, P. Gill, and W. R. C. Rowley, Metrologia **42**, 464 (2005).
25. The clock's frequency was traced to UTC(TL) via the flying clock method; UTC: Coordinated Universal Time.
26. Terasic Inc., model: DE0-NANO; cost 100 USD at 2020.
27. P. Fendel, S. D. Bergeson, T. Udem, and T. W. Hänsch, Opt. Lett. **32**, 701 (2007).
28. R. Boyd, *Nonlinear Optics*, 3rd ed. (Academic Press, 2008).
29. J. Ye, S. Swartz, P. Jungner, and J. L. Hall, Opt. Lett. **21**, 1280 (1996).
30. K. W. Martin, G. Phelps, N. D. Lemke, M. S. Bigelow, B. Stuhl, M. Wojcik, M. Holt, I. Coddingtom, M. W. Bishop, and J. H. Burke, Phys. Rev. Appl. **9**, 014019 (2018).